

Sea ice extent and seasonality for the Early Pliocene northern Weddell Sea

Mark Williams^{a,b,*}, Anna E. Nelson^c, John L. Smellie^{a,c}, Melanie J. Leng^d, Andrew L.A. Johnson^e,
Daniel R. Jarram^a, Alan M. Haywood^f, Victoria L. Peck^c, Jan Zalasiewicz^a, Carys Bennett^a, Bernd
R. Schöne^g

^a*Department of Geology, University of Leicester, Leicester, LE1 7RH, UK*

^b*British Geological Survey, Keyworth, Nottingham, NG12 5GG, UK*

^c*British Antarctic Survey, Geological Sciences Division, High Cross, Madingley Road, Cambridge, CB3
0ET, UK*

^d*NERC Isotope Geosciences Laboratory, British Geological Survey, Keyworth, Nottingham, NG12 5GG, UK*

^e*Geographical, Earth and Environmental Sciences, School of Science, University of Derby, Kedleston Road,
Derby, DE22 1GB, UK*

^f*School of Earth and Environment, University of Leeds, Leeds, LS2 9JT, UK*

^g*Department of Applied and Analytical Palaeontology, Earth System Science Research Centre, Institute of
Geosciences, University of Mainz, Johann-Joachim-Becherweg 21, 55127 Mainz, Germany*

*Corresponding author. E-mail address: mri@le.ac.uk (M. Williams)

Abstract

Growth increment analysis coupled with stable isotopic data ($\delta^{18}\text{O}/\delta^{13}\text{C}$) from Early Pliocene (ca 4.7 Ma) *Austrochlamys anderssoni* from shallow marine sediments of the Cockburn Island Formation, northern Antarctic Peninsula, suggest these bivalves grew through much of the year, even during the coldest parts of winter recorded in the shells. The high frequency fluctuation in growth increment width of *A. anderssoni* appears to reflect periodic, but year-round, agitation of the water column enhancing benthic food supply from organic detritus. This suggests that *Austrochlamys* favoured waters that were largely sea ice free. Our data support interpretation of the Cockburn Island Formation as an interglacial marine deposit and the previous hypothesis that *Austrochlamys* retreated from the Antarctic as sea ice extent expanded, this transition occurring during climate cooling in the Late Pliocene. Our data question climate models that show extensive sea ice in the Weddell Sea during the Early Pliocene.

Keywords: Pliocene, Antarctic, bivalves, seasonality, sea ice, climate

29

30 **1. Introduction**

31 The Pliocene Epoch (5.3 to 2.6 Ma) spans a time when the Earth experienced a transition from
32 relatively warm conditions to a cooling climate that heralded the high magnitude glacial-interglacial
33 oscillations of the Pleistocene Epoch (Haywood et al., 2009). The warm interglacial climates of the
34 Pliocene may be plausible comparative scenarios for interpreting the path of future climate warming
35 during the 21st century (Jansen et al., 2007; Haywood et al., 2009). Whilst overall global climate
36 may have been 2-3°C warmer during the ‘mid Piacenzian warm interval’ (= ‘mid Pliocene warm
37 period’ of earlier papers), climate at high latitudes is modelled to have been much warmer than
38 today (Haywood et al., 2007 and references therein). Given the significance of a warming 21st
39 century global climate and its influence on high latitude sea surface temperatures and sea ice extent,
40 it is important to develop proxies that can ground-truth models of high latitude regions during the
41 Pliocene (e.g. Dowsett, 2007, fig. 6).

42 Bivalves preserve a signal of marine seasonality (e.g. water temperature, upwelling, food
43 supply) in their carbonate geochemistry and skeletal morphology (e.g. Jones and Quitmyer, 1996;
44 A. Johnson et al., 2000, 2009; Schöne et al., 2003, 2005). These signals have been used to provide
45 climate information across a range of palaeolatitudes (e.g. Williams et al., 2009a). Antarctic
46 Peninsula Neogene fossil bivalves have received detailed taxonomic and environmental appraisal
47 (e.g. Jonkers et al., 2002; Jonkers, 2003) but they have not been used to assemble a record of
48 seasonality. Nevertheless, Berkman et al. (2004) have presented a cogent argument, based on
49 morphological and sedimentological analyses, which suggests that the retreat of *Chlamys*-like
50 bivalves from the Antarctic resulted from increasing sea ice cover during the climate cooling of the
51 Late Pliocene.

52 The pectinid bivalve *Austrochlamys anderssoni* occurs commonly in rocks of Late Miocene
53 through Pliocene age on the northern Antarctic Peninsula. *Austrochlamys anderssoni* is ideal for
54 investigation of palaeoseasonality as specimens are large, often reaching greater than 10 cm from

55 umbo to margin in adults, and record a number of seasons of growth. In addition, the width of
56 individual growth increments in *A. anderssoni* is easy to measure (mm-scale), and they are
57 correspondingly easy to sample for geochemical analysis. Here we analyze ontogenetic patterns in
58 *A. anderssoni* to test for the extent of sea ice in the northern Weddell Sea during a warm interval of
59 the Early Pliocene. We test two possible marine scenarios: 1), that there was extensive winter sea
60 ice with no planktonic food-supply, no re-suspension of detrital food and therefore limited or no
61 bivalve growth, an environment suggested by some climate models (see Fig. 1); and 2), no winter
62 sea ice with bivalve growth continuing via a supply of periodically re-suspended organic detritus
63 via water column agitation. We use stable oxygen and carbon isotopes to define seasonal intervals
64 during the growth of *A. anderssoni* and to estimate seasonal temperature variation: we then use
65 growth increment data as a proxy to interpret benthic food supply and sea ice extent.

66

67 **2. Geological setting**

68 The James Ross Island Volcanic Group (JRIVG) dominates the outcrop geology of James Ross
69 Island, Vega Island and several small islands including Cockburn Island, in the northern Weddell
70 Sea, east of the Antarctic Peninsula (Fig. 2). The volcanic rocks unconformably overlie relatively
71 unconsolidated Cretaceous marine deposits. About 10 million years of late Neogene and Quaternary
72 history is recorded in the JRIVG (Smellie et al., 2006a, b, 2007, 2008, 2009; Hambrey et al., 2008).
73 Sedimentary rocks in the JRIVG are dominated by diamictite conglomerate and minor sandstone
74 (Smellie et al., 2006a; Hambrey et al., 2008; Nelson et al., 2009). Two sedimentary formations have
75 been defined, the interglacial marine Cockburn Island Formation (Jonkers, 1998a, b) and the glacial
76 Hobbs Glacier Formation (Pirrie et al., 1997). Fossils have been recovered from both of these
77 formations, and in addition rare asterozoan trace fossils are preserved in marine-deposited volcanic
78 tuffs (Williams et al., 2006; Nelson et al., 2008). The JRIVG represents an important and largely
79 unexploited archive of late Neogene fossil and geochemical data for reconstructing past climate and
80 seasonal regimes at high southern latitude.

81 The richest Neogene fossil assemblages in the JRIVG are those of the interglacial marine
82 Cockburn Island Formation, which contains abundant large molluscs, especially *Austrochlamys*
83 (*Zygochlamys* of Jonkers et al., 2002; see Jonkers, 2003 for a detailed taxonomic appraisal). The
84 glacimarine deposits of the Hobbs Glacier Formation contain similar macrofossil assemblages, are
85 dominated by molluscs (including *Austrochlamys*), but also contain older material reworked from
86 the Cretaceous (Smellie et al., 2006a). Collectively these fossils occur in strata of Late Miocene (ca
87 6 Ma) through to Pleistocene age (ca 2 Ma). Detailed analysis of the JRIVG has identified three
88 intervals of relative warmth in the northern Peninsula region, when volcanic rocks were erupted into
89 a marine environment (Smellie et al., 2006a, fig. 6). Radiometric ($^{40}\text{Ar}/^{39}\text{Ar}$) dates from the
90 volcanic rocks, together with $^{87}\text{Sr}/^{86}\text{Sr}$ chronology from the molluscs in the intervening glacimarine
91 and interglacial marine rocks have produced a well-resolved stratigraphy which constrains the
92 warm intervals to 6.5 to 5.9, 5.03 to 4.22, and ca 0.88 Ma. The *Austrochlamys* material we study
93 here, from the second of these warm intervals, is dated at 4.66 +0.17/-0.24 Ma by McArthur et al.
94 (2006).

95

96 **3. Provenance of bivalve material on Cockburn Island**

97 The *Austrochlamys* bivalve material is sourced from three localities on the east side of Cockburn
98 Island referred to in BAS archives as DJ.851, DJ.852 and DJ.853 (Fig. 2). This material was
99 collected by H.A. Jonkers in 1996 though the island had been visited on several occasions dating
100 back to 1906 (Jonkers, 1998a). The Cockburn Island Formation forms small outcrops at a number
101 of localities on the island and Jonkers recognised a western ‘proximal’ or ‘littoral’ facies and an
102 eastern ‘distal’ facies. Based on the gradient atop the island he estimated the latter, bivalve-bearing
103 facies to represent original water depths no greater than 100 m. Fossils associated with the bivalves
104 include echinoids, gastropods, brachiopods, serpulids and rare possible penguin bones. The precise
105 stratigraphical relationships of the bivalve material from the three localities documented here is
106 difficult to discern, but they are clearly from the same substratum.

107

108 **4. *Austrochlamys* as a palaeoenvironmental index of Antarctic shelf waters in the late Neogene**

109 *Austrochlamys* is an epibenthic pectinid bivalve genus comprising six species whose distribution is
110 restricted to the Antarctic and sub-Antarctic region, with one extant species known from South
111 America (Jonkers, 2003; Quilty et al., 2004). The earliest *Austrochlamys* occur in Oligocene
112 deposits of King George Island (for a summary of fossil occurrences see Berkman et al., 2004).
113 Sub-fossil material is also known from as far north as southern New Zealand (Auckland Islands,
114 Dijkstra and Marshall, 2008). Fossils of *Austrochlamys* are prolific and widespread in strata of Late
115 Miocene through Pliocene age of the Hobbs Glacier and Cockburn Island formations and often are
116 very well preserved (Fig. 3), with specimens articulated even when they occur in glacimarine
117 deposits (Nelson et al., 2009). Jonkers et al. (2002) believed this was a function of minimal
118 transport with the bivalves preserved virtually *in situ*. *Austrochlamys* of the Hobbs Glacier and
119 Cockburn Island formations belong to the species *A. anderssoni* (see Jonkers, 2003), thought to be a
120 byssally attached epibenthic form (Berkman et al., 2004, p. 1845). Although these bivalves are
121 believed to have occupied water depths not greater than 100 m (Jonkers, 1998a; Jonkers et al.,
122 2002), sometimes they occur as transported fragmentary specimens in strata that may have been
123 deposited at greater water depths (Jonkers et al., 2002, p. 586).

124 *Austrochlamys* is a significant indicator of palaeoenvironment for the Antarctic (Berkman et
125 al., 2004). Modern *Austrochlamys natans* occur in the high energy sub-littoral and littoral zones of
126 southern Chile and Argentina, as far south as Bahia Orange (Dijkstra and Köhler, 2008). Modern
127 sea surface temperatures in southernmost South America range between about 5 to 10°C (NOAA
128 monthly global SST plot archive at: http://www.emc.ncep.noaa.gov/research/cmb/sst_analysis/). As
129 well as living at shallow depths *Austrochlamys* is recovered from greater depths, and for example
130 the holotype of *A. natans* was recovered from 125 m in the Magellan Strait (see Dijkstra and
131 Marshall, 2008). Seawater temperatures in southernmost South America (between 52 to 56°S) at
132 depth 125 m range between about 4 to 8°C annually, and at 500 m are between 4 to 6°C (NODC

133 World Ocean Atlas, Monthly Mean one degree sea temperatures at:
134 <http://apdrc.soest.hawaii.edu/las/servlets/dataset>). Berkman et al. (2004) have argued that the
135 presence of *Austrochlamys* in Antarctic fossil assemblages suggests similar conditions to modern
136 southernmost South America, and in particular, much reduced sea ice extent. Jonkers (1998a) also
137 suggested a sea ice free environment for the Cockburn Island Formation, based on the presence of
138 barnacles in his littoral facies and the absence of ice-rafted debris. Opal depositional rates, which
139 are linked to biological productivity, are conspicuously enhanced in the Early Pliocene, between 5.2
140 and 3.1 Ma, signifying much-reduced sea ice cover (Hillenbrand and Fütterer, 2002; Pudsey, 2002).
141 Although microfossil assemblages found in the ODP Leg 178 drift sediments show no evidence of
142 significantly warmer surface water temperatures than today (Hillenbrand and Fütterer, 2002), Hepp
143 et al. (2006) have suggested open ocean conditions in the warm Early Pliocene, even during
144 glacials. In addition, diatom evidence from ODP site 1165 (in the Southern Ocean at 64.384°S)
145 reported by Whitehead and Bohaty (2003) gives mean annual temperatures at 4°C, and the absence
146 of ice-rafted debris in the Cockburn Island Formation (Jonkers, 1998a) also suggests warmer
147 conditions than present.

148 Modern coastal environments of James Ross Island and other Antarctic regions, where
149 seasonal sea ice is prevalent, are characterised by the slow-growing, thin-shelled scallop
150 *Adamussium colbecki* (Berkman et al., 2004). This bivalve is thought to have originated in deeper
151 water and to have migrated on to the shelf as conditions cooled during the Late Pliocene.
152 *Adamussium colbecki* lives below sea ice, in conditions that mimic the deep ocean. It effectively
153 replaced *Austrochlamys* as the dominant scallop, which retreated across the Southern Ocean to
154 South America (Berkman et al., 2004). Thus, *Austrochlamys* may provide a proxy of reduced sea
155 ice conditions and more agitated coastal waters around James Ross and Cockburn islands during the
156 Pliocene, a hypothesis that we will test in this paper by examining the growth-increment pattern and
157 geochemical signature of fossil shells.

158

159 **5. Methodology: analysis of bivalve material**

160 Our methodology to understand the growth and habitat of fossil *Austrochlamys* in the Cockburn
161 Island Formation uses three lines of evidence: oxygen isotopes to determine seasonality and the
162 approximate temperature of the water in which the bivalves were living; carbon isotopes to
163 determine metabolic rates and food supply during growth; and growth increments to assess the
164 pattern of growth. Relating these different data sources is a means of providing a detailed picture of
165 the environmental setting of *Austrochlamys* in the late Neogene coastal waters of the Antarctic.

166

167 *5.1 Geochemical analyses*

168 Only well-preserved fossil material has been analysed. Neogene shells of *Austrochlamys* from the
169 Antarctic Peninsula that we interpret as being pristine show no variation in composition that is
170 detectable under Scanning Electron Microscopy (with EDX analysis). With the exception of a few
171 specimens, the shell lamellae have no visible cement overgrowths or recrystallisation. The calcitic
172 shell lamellae (confirmed by XRD analysis of 3 shell fragments) are non-luminescent to weakly
173 luminescent under cathodoluminescence, indicating no diagenetic cements are present. One
174 specimen has a diagenetic cement overgrowth on the external surface of the valve as bladed calcite
175 crystals, which are strongly luminescent (Fig. 4), and this specimen has been excluded from the
176 isotopic analysis. Many shells have a fine layer of carbonate-cemented clay material adhering to the
177 outer surface of the shell. Before drilling for geochemical analysis, this extraneous material was
178 removed by gentle scrubbing and immersion of the shell in a bath of 5% HCl followed by washing
179 with de-ionised water. After this treatment the shells looked pristine with the majority of the
180 sediment removed and the growth increments clearly showing. The growth increments of
181 *Austrochlamys* are large and easy to drill and it is possible to obtain sufficient material from each,
182 whilst avoiding remaining adherent sediment. Shells representing several years of growth (e.g.
183 DJ.851.159, DJ.851.160 and DJ.853.1) were selected for analysis. Some 250 growth increments
184 from three shells have been sampled for calcite and analysed for stable carbon and oxygen isotopes

185 (Figs 3, 6). Approximately 30-100 micrograms of carbonate have been used for each isotope
 186 analysis using a GV IsoPrime mass spectrometer plus Multiprep device. Isotope values ($\delta^{13}\text{C}$, $\delta^{18}\text{O}$)
 187 are reported as per mil (‰) deviations of the isotopic ratios ($^{13}\text{C}/^{12}\text{C}$, $^{18}\text{O}/^{16}\text{O}$) calculated to the
 188 VPDB scale using a within-run laboratory standard calibrated against NBS standards. Analytical
 189 reproducibility of the standard calcite (KCM) run with these samples was 0.02‰ for $\delta^{13}\text{C}$ and
 190 0.04‰ for $\delta^{18}\text{O}$. Values for oxygen isotopes have been converted to sea palaeotemperatures using
 191 the equation of O'Neil et al. (1969), $T = 16.9 - 4.38(\delta^{18}\text{O}_c - \delta^{18}\text{O}_{\text{sw}}) + 0.10(\delta^{18}\text{O}_c - \delta^{18}\text{O}_{\text{sw}})^2$. A.
 192 Johnson et al. (2000) have demonstrated good calibration between actual sea temperatures and
 193 reconstructed sea temperatures using this equation applied to North Sea modern and sub-fossil
 194 *Aequipecten*. For comparison we have also calculated palaeotemperatures using a modified form of
 195 the Craig (1965) equation given in Leng and Marshall (2004), $T = 16 - 4.14(\delta^{18}\text{O}_c - \delta^{18}\text{O}_{\text{sw}}) +$
 196 $0.13(\delta^{18}\text{O}_c - \delta^{18}\text{O}_{\text{sw}})^2$: typically this makes palaeotemperature estimates warmer by about 0.5 to
 197 0.8°C (see Table 1).

198

199 5.2 Assessing seawater isotopic composition

200 Implicit in calculations of palaeotemperature from the $\delta^{18}\text{O}$ of *Austrochlamys* calcite is an
 201 assessment of the isotopic composition of the seawater ($\delta^{18}\text{O}_{\text{sw}}$) in which the bivalves were living.
 202 Surface seawater $\delta^{18}\text{O}$ in the Weddell Sea today is between 0 and -0.5‰ (Schmidt et al., 1999).
 203 Mackensen (2002) gives a mean value of -0.37‰ for Antarctic Surface Water in the southern
 204 Weddell Sea. Oceanographic conditions in the Weddell Sea have been summarized by Whitehouse
 205 et al. (1996), who showed summer to winter temperature variation between +1.99 and -0.10°C,
 206 with salinity greater in winter time (33.87 to 34.05 psu) than in summer (33.81 to 33.86 psu). The
 207 flux of isotopically light glacial meltwater into the northern Weddell Sea around James Ross Island
 208 during the summer months affects the $\delta^{18}\text{O}$ of surface water. Although there are no detailed studies
 209 of meltwater flux around James Ross Island, these effects are well constrained for surface water on
 210 the western Antarctic Peninsula region in Marguerite Bay at 68°S (Meredith et al., 2008). The

211 setting of Marguerite Bay is different from that of the Weddell Sea in that $\delta^{18}\text{O}_{\text{sw}}$ values in the
212 western peninsula region are lower for surface waters (between -0.5 to -1‰ ; see Schmidt et al.,
213 1999). However, the north end of Marguerite Bay is covered by winter sea ice for several months,
214 so that it provides a useful comparison for seasonal fluxes of sea ice and glacial meltwater into the
215 modern James Ross Island area, where sea ice also forms during the winter months. In Marguerite
216 Bay as much as 5% of the near-surface ocean is glacial meltwater: sea ice-melt accounts for a much
217 smaller percentage (*ca* 1%). The effects of seasonal sea ice-melt on the $\delta^{18}\text{O}_{\text{sw}}$ are minimal
218 (Meredith et al., 2008, p. 314) but those of glacial ice-melt are much more significant as high
219 latitude ice has very low $\delta^{18}\text{O}$ (Mackensen, 2002; Meredith et al., 2008). In Marguerite Bay surface
220 waters are isotopically lightest during the summer months, with values as low as -0.9‰ (compared
221 with higher values of -0.1‰ for deeper water below 300 m). During winter months the $\delta^{18}\text{O}$ of
222 surface waters is about -0.5‰ , still much lower than deeper waters and indicating that significant
223 quantities of meteoric water remain in the upper water column throughout the year.

224 Our estimates of palaeotemperature from *Austrochlamys* have assumed an initial surface
225 $\delta^{18}\text{O}_{\text{sw}}$ value of -0.2‰ . This is a mean value sourced from a climate model study of the Early
226 Pliocene (Lunt et al., 2008) and is similar to modern surface conditions in the Weddell Sea
227 (Schmidt et al., 1999; Mackensen, 2002). For calculations of $\delta^{18}\text{O}_{\text{sw}}$ from the model see Appendix
228 1. There is considerable evidence for the persistence of an Antarctic Peninsula Ice Sheet even
229 during warm phases of the late Neogene (Smellie et al., 2009; J. Johnson et al., 2009; Nelson et al.,
230 2009), though sea ice cover in this region may have been much more limited (Berkman et al.,
231 2004). Thus, fluxes of meltwater such as those into Marguerite Bay may have characterized the
232 northern Weddell Sea region during warm interval summers, and may have kept surface waters
233 isotopically light throughout the year, with $\delta^{18}\text{O}$ values lowest during the summer. For this reason,
234 we have also calculated palaeotemperatures using higher and lower values of $\delta^{18}\text{O}_{\text{sw}}$ (0 to -0.4‰) to
235 reflect seasonal (winter-summer) variation (see Table 1).

236

237 5.3 Growth increment analysis

238 *Austrochlamys* grows by a series of increments that are visible on the shell surface (Fig. 3). These
239 increments result from the advance of the mantle over the ventral margin to effect extension of
240 extrapallial fluid and precipitation of calcite to the shell edge. In scallops, as in other bivalves,
241 large-scale mantle advance and shell-size increase is dependent on the environmental conditions
242 which facilitate cell division and growth. However, under such conditions, shell extension is fairly
243 regularly interrupted for short periods through retraction of the mantle edge, resulting in an
244 incremental pattern of shell growth which is clearly marked by commarginal ridges on the external
245 surface (Clark, 1974, 2005). The individual (microgrowth) increments may be over 1 mm in width
246 in *Austrochlamys* (Fig. 5), which is exceptionally large amongst scallops (cf. Clark, 2005; Owen et
247 al., 2002b; A. Johnson et al., 2009). Overall periods of growth may be succeeded by sudden and
248 sharp reductions in calcite precipitation, and the shell is therefore marked by a distinct band known
249 as a ‘growth line’. These lines may represent suspension of growth associated with seasonal
250 temperature extremes, wave action, reproduction (Dame, 1996, p. 58) or disturbance (e.g. Adam,
251 1990). In *Austrochlamys* from the Cockburn Island Formation growth lines are developed on many
252 shells with varying degrees of prominence (Fig. 3).

253 To measure growth increments precisely, scaled photographic images of *Austrochlamys*
254 were imported into the software Panopea (© Peinl and Schöne, 2004). This enables point-to-point
255 measurements of growth increment widths and reference features, and outputs a precise width of
256 these structures. The factors behind the rate of growth of *Austrochlamys* cannot be differentiated by
257 growth increments alone (see Jones and Quitmyer, 1996), but coupled to $\delta^{13}\text{C}$ and $\delta^{18}\text{O}$ profiles (see
258 A. Johnson et al., 2000, 2009) it is possible to make inferences about control mechanisms such as
259 food supply and water temperature.

260

261 6. Results and interpretation

262 6.1 Oxygen isotopes and palaeotemperature

263 The three shells we have analysed for stable isotopes collectively record about seven summer-
264 winter cycles of growth (Fig. 6), with an overall reconstructed temperature range from -1 to +3.5°C
265 (using the O'Neil et al., 1969 equation), or slightly higher minimum and lower maximum
266 temperatures if higher winter and lower summer $\delta^{18}\text{O}_{\text{sw}}$ values are used (Table 1). We do not
267 suggest that this represents the entire range of climate for the Cockburn Island Formation, but it
268 does provide the first quantifiable evidence of sea temperature seasonality for about seven years in
269 this region from the late Neogene. The two shells from locality DJ.851 show similar temperature
270 profiles, while that from locality DJ.853 shows the warmest summer values (Fig. 6, Table 1). These
271 two bivalve-bearing localities are separated by about 300 m along a north-south transect on the east
272 side of the island (Fig. 2) and while the bivalves are from the same substratum, they may represent
273 molluscs living 100s of years apart.

274 Isotope analysis of shell DJ.851.159 shows a signal of seasonality in water temperature over
275 three cycles of summer-winter growth (Fig. 6). During this interval (using an annual mean $\delta^{18}\text{O}_{\text{sw}}$ of
276 -0.2‰ and the O'Neil et al., 1969 equation), sea temperatures between -1.1 and $+2.5^\circ\text{C}$ are
277 suggested. This range of temperature variation (*ca* 3.6°C) is similar to the present mean intra-annual
278 range in surface waters of the Weddell Sea (see Whitehouse et al., 1996). It is also similar to the
279 seasonal temperature variation at the sea surface predicted by an Early Pliocene climate model,
280 giving values of -1.69°C for winter (July) and $+3.08^\circ\text{C}$ for summer (February) at depth 0-5 m (Lunt
281 et al., 2008). At depth (95-113 m) seasonality from the model is just -0.69 to -0.52°C . This
282 supports the notion that the *Austrochlamys* of the Cockburn Island Formation were living at shallow
283 depth, recording much of (or the entire) surface seasonality, and were well above the maximum
284 depth of 100 m speculated on by Jonkers et al. (1998a, 2002).

285 The use of a single mean annual value for $\delta^{18}\text{O}_{\text{sw}}$ in our calculations shown in Figure 6 may
286 be unjustified (and lead to over- or underestimates of palaeotemperature) in that it assumes no large
287 change in glacial meltwater flux to this region of the northern Weddell Sea between summer and
288 winter. Calculating sea temperatures for shell DJ.851.159 using a winter value of 0‰ for $\delta^{18}\text{O}_{\text{sw}}$

289 gives a minimum water temperature of -0.4°C , close to that recorded today. Using a summer value
290 of -0.4‰ for $\delta^{18}\text{O}_{\text{sw}}$ gives a maximum temperature of about 2°C (Table 1). This seasonal range in
291 $\delta^{18}\text{O}_{\text{sw}}$ is justified by modern data from Marguerite Bay (see Meredith et al., 2008 and above).

292 Forty analyses from shell DJ.851.160 produce estimated sea temperatures similar to those of
293 shell DJ.851.159, with a minimum just below 0°C and a maximum of 1.8°C (for $\delta^{18}\text{O}_{\text{sw}} = -0.2\text{‰}$,
294 see Fig. 6, see also Table 1). In contrast, shell DJ.853.1, which also records about three cycles of
295 summer-winter growth (*ca* 100 increments drilled), provides sea temperatures between 0.5 and
296 3.5°C (for $\delta^{18}\text{O}_{\text{sw}} = -0.2\text{‰}$, Fig. 6). Given that these shells are from two different localities, the
297 latter hints that a very detailed record of changing regional climate may be stored in these fossils.

298 Modern temperature beneath the sea ice during winter months in the Weddell Sea is close to
299 0°C (Whitehouse et al., 1996; cf. with similar sea temperatures in Marguerite Bay reported by
300 Meredith et al., 2008, p. 312), suggesting that our estimates of winter temperature in shells from
301 locality DJ.851 may be too cool for the Early Pliocene. Although the overall degree of seasonal sea
302 temperature change appears similar to present (Table 1), we cannot be sure that our reconstructed
303 temperatures reflect absolute values. However, given a winter temperature of -1.1°C from bivalve
304 DJ.851.159, they must represent near minimum values. Recalculating palaeotemperatures using the
305 modified form of the ‘Craig (1965)’ equation (see Table 1) gives a slightly elevated minimum
306 temperature of -0.3°C for shell DJ.851.159, close to the modern minimum values recorded by
307 Whitehouse et al. (1996).

308 As well as the problem of assessing initial $\delta^{18}\text{O}_{\text{sw}}$ some bivalves are known to exhibit vital
309 effects. Thus, experimental work on *Pecten maximus* shows deviations of shell $\delta^{18}\text{O}$ from
310 equilibrium of $+0.6\text{‰}$, equivalent to a temperature interpretation $2\text{--}3^{\circ}\text{C}$ colder than actual (Owen et
311 al., 2002a). With our available data we cannot assess whether vital effects have influenced the $\delta^{18}\text{O}$
312 of *Austrochlamys calcite*, but it is feasible that our minimum and maximum estimates of sea
313 temperature are colder than actual, and that sea temperatures were above zero throughout the year at
314 the time the Cockburn Island Formation was being deposited. This is suggested by sea temperature

315 values from the shell at locality DJ.853 that show a minimum above 0°C (Fig. 6, Table 1), and by
316 our growth increment data (see below).

317

318 6.2 Carbon isotopes and planktonic productivity

319 The $\delta^{13}\text{C}$ signature of bivalves is influenced by the isotopic composition of the dissolved inorganic
320 carbon (DIC) in seawater, its major controls being local phytoplankton productivity (removing ^{12}C),
321 local respiration (returning ^{12}C) and influxes of isotopically more negative deep ocean water or
322 freshwater (Krantz et al., 1987). Thus, bivalves living close to upwelling zones can exhibit marked
323 changes in $\delta^{13}\text{C}$ (Jones and Allmon, 1996) whereas those living away from such zones may exhibit
324 a much smaller degree of variation, less than 1‰ (A. Johnson et al., 2000, 2009). The $\delta^{13}\text{C}$ may
325 also reflect a kinetic effect. This results in a depletion of both ^{18}O and ^{13}C in carbonates
326 (McConnaughey et al., 1997; Owen et al., 2002a). In contrast, metabolic (respiration) effects will be
327 reflected in depletions in shell $\delta^{13}\text{C}$ (McConnaughey and Gillikin, 2008) which are not
328 accompanied by simultaneous changes in shell $\delta^{18}\text{O}$. Thus, the two mechanisms can be
329 differentiated in isotopic profiles of bivalves.

330 The carbon isotope signature of *A. anderssoni* suggests both metabolic and oceanographic
331 controls, but not kinetic effects. Carbon isotope values are lowest through the first annual cycle of
332 temperature variation recorded in shell DJ.851.159 (*ca* 1.4‰), perhaps related to high metabolic
333 rate in a young specimen. The carbon signature is a little higher through the second cycle of
334 temperature variation recorded in shell DJ.851.159 (*ca* 1.7‰), and then is variable into the third
335 cycle (from *ca* 1.2 to nearly 2‰). However, the two peaks of highest carbon values (at about 2‰)
336 correlate with summer temperature maxima determined from analysis of $\delta^{18}\text{O}$ (Fig. 6), and suggest
337 a phytoplankton control, influenced by a summer bloom. There are no areas of the shell DJ.851.159
338 profile where oxygen and carbon show depletion in tandem, and we interpret this as being evidence
339 of minimal or no kinetic effects. A very similar pattern of highest $\delta^{13}\text{C}$ (about 2‰) associated with
340 summer temperature is also preserved in shell DJ.851.160 (Fig. 6). Peak highest values of $\delta^{13}\text{C}$ also

341 coincide with warmest estimated sea temperatures in bivalve DJ.853.1. Here though, peak highest
342 $\delta^{13}\text{C}$ values (of 2.4‰) are greater than in the two bivalves from locality DJ.851, suggesting that
343 increased water column productivity might have been influenced by the warmer overall
344 temperatures apparently experienced by bivalve DJ.853.1.

345 Conceivably, more upwelling of deep ocean water in winter-time could produce the
346 characteristic low $\delta^{13}\text{C}$ patterns that correlate with the highest $\delta^{18}\text{O}$ in the three shells analysed (Fig.
347 6). Differences in wind strength between summer (weaker) and winter (stronger) could account for
348 this, but these differences could not have had an effect if the sea was ice-covered in winter.

349

350 *6.3 Growth increments and the availability of benthic food*

351 All of the bivalves measured show patterns in growth involving clusters of broader and narrower
352 increments (Fig. 5). The initial (umbonal) region of each shell bears increments which are too
353 narrow or ill-defined to be measured (Fig. 3). This is typically over the first 2-3 cm of well-
354 preserved shells. Thus, we have been unable to assess growth patterns for the earliest stages of
355 development in *Austrochlamys* and it should be noted that the graphs do not represent the same
356 growth increment interval between bivalves (see Fig. 3 for position of growth measured on each
357 shell). For those increments that can be measured, there is a wide range of variation in width both
358 within and between shells, varying from 0.09 mm (DJ.852.1) to *ca* 1.7 mm (DJ.851.3). Some
359 specimens clearly have broader growth increments overall: thus, 5 cm of shell growth can be
360 achieved over 60 (e.g. DJ.851.3), 76 (DJ.851.80) or 93 increments (DJ.851.159). The number of
361 increments between a peak and a trough in the growth of *Austrochlamys* varies from about 3 to 14,
362 with no discernible increase in frequency from younger to older specimens (Fig. 5).
363 Notwithstanding the growth lines that represent probable growth breaks, analysis of growth
364 cumulatively suggests that while *Austrochlamys* is growing, growth rate remains similar, with no
365 significant reduction during colder periods (see Fig. 6).

366 The annual cycles in environmental variables (e.g. sea temperature and phytoplankton
367 productivity) determined from stable oxygen and carbon isotope analyses correspond to growth
368 intervals involving from 24 to 38 increments on shell DJ.851.159, with winter troughs at increments
369 19, 57 and beyond 81 (and summer highs at increments 1, 39 and 75 respectively). The winter-
370 summer signal from the isotopes is clearly independent of the growth variation exhibited by the
371 increments, which have a much higher frequency of change (Fig. 6) and were likely controlled by
372 other factors. In addition, the seasonal temperature signal does not appear to bear any close
373 relationship to the distinctive growth lines of shell DJ.851.159, at least one of which appears to be
374 associated with marginal shell damage (see Figs 3, 6) and therefore perhaps disturbance. Shell
375 DJ.851.160, from the same locality as DJ.851.159, confirms this pattern, with growth increment
376 variation of similar degree in both summer and winter, and a growth line in the part of the shell
377 drilled for stable isotopes which is synchronous with rising temperatures, probably towards the end
378 of a winter cycle (Fig. 6).

379 In contrast shell DJ.853.1, from the northern-most pectinid-bearing locality on Cockburn
380 Island (Fig. 2) shows a different pattern of growth to those shells from locality DJ.851. In this shell
381 two growth lines do equate to intervals of temperature lows (Fig. 6), though not to the final low
382 temperature interval (beyond increment 90). From increment 1 to 59 there is no apparent summer-
383 winter variation in overall growth rate when the bivalves are growing, with peaks and troughs in
384 increment width occurring with a higher frequency than the peaks and troughs in temperature
385 variation (fig. 6). The first weak growth line appears to come towards the end of a winter cycle, and
386 is associated with a temperature low. But this growth break appears to have been of short duration
387 as there is a substantial interval of winter prior to this (Fig. 6). It occurs in that part of the shell
388 where the $\delta^{13}\text{C}$ signal indicates a rapid increase in water column productivity, and therefore the
389 growth line probably formed at, or just prior to the beginning of spring-summer. The second growth
390 line, beginning at about increment 58, is stronger and corresponds to a temperature low. Here there
391 is clear evidence for a slowing of growth (from increment size measurements, Fig. 6), and this part

392 of the shell is also associated with a rapid change to lower $\delta^{13}\text{C}$ that may record the onset of winter.
393 The isotope record is missing through about 5 to 6 increments as these were too narrow to drill, and
394 so the winter temperature minimum has not been determined. The increments immediately
395 following the growth line show rapid temperature rise into summer (Fig. 6). Nevertheless, the
396 temperature low associated with this growth line (and apparent growth cessation) was well above
397 zero at the time growth slowed (Fig. 6), and is in line with winter temperature values elsewhere in
398 this shell where growth continued. We therefore suggest that this growth break might be associated
399 with shell disturbance, rather than with growth cessation from low temperature. Shell DJ.853.1
400 records a second season of summer growth with a maximum estimated temperature of 3.5°C at
401 increment 72, and a final period of presumed winter growth with temperatures about 1.5°C beyond
402 increment 88 (Fig. 6). There is no distinctive growth line associated with the beginning of this last
403 interval of ‘cooler’ temperatures, and increment analysis indicates that growth continued at a
404 similar pace irrespective of whether temperatures were ‘warm’ or ‘cool’ (Fig. 6).

405 Conventional wisdom interprets the growth patterns of bivalves in terms of summer to
406 winter variation, but Jones and Quitmyer (1996) have demonstrated convincingly that there may be
407 a decoupling between growth rate and temperature in bivalves. The growth-increment patterns in
408 the shells analysed for stable isotopes from the Cockburn Island Formation (Figs 3, 6) are closely
409 comparable to those of Holocene *Aequipecten* from the North Sea (A. Johnson et al., 2009) – that is,
410 there is no seasonal pattern that can be tied with the palaeotemperature profile reconstructed from
411 stable oxygen isotope evidence. Neither is there any correspondence to the pattern of planktonic
412 productivity inferred from carbon isotope evidence. In natural populations of the scallop
413 *Aequipecten* growth is probably tied with benthic food supply, particularly with the availability of
414 detrital organic material. This increases during periods of water column agitation. Growth in the
415 infaunal bivalve *Arctica* appears to be under a similar control (Schöne et al., 2003, 2005; Witbaard,
416 1996) and the correlation between increment size in Pliocene *Flabellipecten steamsi* from the Gulf
417 of California and tidal patterns in this area (Clark, 2005) is also accountable to re-suspension and

418 advection of detrital food by tidal currents. In the Weddell Sea, present winter sea ice-cover
419 suppresses movement in the water column during the winter months. Therefore, if sea ice was
420 extensive during the winter months of the Early Pliocene, this would have resulted in reduced
421 agitation of the water column, reduced food supply, and a clear seasonality in growth for *A.*
422 *anderssoni*. Moreover, there should be less short-term variation in winter than in summer (when the
423 water column would be more agitated), but this is not the case. The growth increment data from *A.*
424 *anderssoni* is consistent with the proposal of Berkman et al. (2004) that there was reduced (or no)
425 sea ice in Early Pliocene coastal marine settings occupied by *Austrochlamys*. The data also imply
426 that *Austrochlamys* has retreated from the Antarctic as the extent of sea ice grew, probably during
427 cooling in the Late Pliocene to Pleistocene. These Antarctic coastal zones today are colonised by
428 the slow-growing *Adamussium colbecki*, a bivalve that originated in deeper waters that are
429 mimicked by living below sea ice (see Berkman et al., 2004).

430

431 **7. Marine seasonality and environment on the Antarctic Peninsula during the Early Pliocene**

432 Our data provide a signal of seasonality during warm interglacial phases of Antarctic climate in the
433 late Neogene and allow testing of models of sea ice extent during the Early Pliocene. Growth
434 increment analysis coupled with stable isotope data indicates that sea temperature was not the major
435 influence on growth for *A. anderssoni*. Instead, growth appears to have continued throughout much
436 of the year (even during the coldest parts of winter as recorded in our shells) with a high frequency
437 fluctuation that probably reflects periodic agitation of the water column and enhanced benthic food
438 supply from organic detritus. Such an interpretation differs from the suggestion of Jonkers et al.
439 (2002, p. 587) that the occurrence of *A. anderssoni* in both the Hobbs Glacier (glacial) and
440 Cockburn Island (glacimarine/interglacial) formations indicates its wide environmental tolerance,
441 and that it should therefore not be used solely as an indicator of interglacial (= present-like
442 conditions). Our evidence also suggests that *Austrochlamys* favoured waters that were sea ice-free,
443 and its presence in the Hobbs Glacier Formation may reflect its incorporation into ice toward the

444 end of an interglacial. Ice-proximal glaciomarine debris flows on James Ross Island incorporated
445 well-preserved bivalves and bryozoans, suggesting that ice expansion occurred under warm
446 conditions during the Pliocene, probably towards glacial inception (Nelson et al., 2009). The
447 presence of bivalves in close proximity to the palaeo-coastline supports the hypothesis of a lack of
448 sea ice, despite the presence of advancing terrestrial-based ice on James Ross Island and the
449 Antarctic Peninsula.

450 The range of temperatures recorded by the bivalves is similar to the mean annual sea surface
451 temperature range in this region at present (see Table 1). Using the O'Neil et al. (1969) equation,
452 and assuming no vital effects and that our estimates of $\delta^{18}\text{O}_{\text{sw}}$ approximate reality, the shells that we
453 have analysed show minimum and maximum temperatures to have been between about -1.1 and
454 $+2.5^\circ\text{C}$ for the bivalves of locality DJ.851, and temperatures between 0.5 and 3.5°C for locality
455 DJ.853: the temperature range is slightly warmer if we use the modified form of the Craig (1965)
456 equation (see Table 1) with values of -0.3 to 2.8°C for DJ.851 and 1.1 to 3.7°C for DJ.853. Our
457 growth increment data, coupled with supporting palaeotemperature information, support: the
458 interpretation of the Cockburn Island Formation as an interglacial marine deposit; the notion of
459 reduced sea ice in the Antarctic during the Pliocene (e.g. Whitehead et al., 2005); and the
460 hypothesis of Berkman et al. (2004) that *Austrochlamys* retreated from the Antarctic as sea ice
461 expanded, this transition occurring during climate cooling in the Late Pliocene. Our bivalve data
462 question climate model predictions of extensive sea ice in the Weddell Sea during the Early
463 Pliocene.

464

465 **8. Further work**

466 Our work has demonstrated the potential value of *Austrochlamys* for testing hypotheses of
467 seasonality and sea ice extent for pre-Quaternary time slices in the Antarctic. As both the Hobbs
468 Glacier and Cockburn Island formations bear rich bivalve material over a wider stratigraphical
469 range than we have analysed here, there is great scope for developing a highly resolved proxy for

470 marine palaeoseasonality at these latitudes. Together with the largely unstudied cheilostome
471 bryozoan faunas in the JRIVG – themselves a group of fossils which are excellent proxies for mean
472 annual range of temperature (see Knowles et al., 2009) - a highly resolved record of palaeoclimate
473 through the Late Miocene and Pliocene of the Antarctic Peninsula region may be obtainable.

474

475 **Acknowledgments**

476 The growth increment analysis of *Austrochlamys* was undertaken by Daniel Jarram as part of his final year Masters
477 project at the University of Leicester. This work contributes to the British Antarctic Survey's GEACEP Programme
478 (ISODYN Project - Ice House Earth: Stability or Dynamism), to the British Geological Survey's deep time
479 palaeoclimate project, and to the SCAR ACE Programme (Antarctic Climate Evolution). We acknowledge support from
480 the NERC Isotope Geosciences Facilities Steering Committee (grant IP/936/1106). We thank Captain Bob Tarrant and
481 the officers and crew of HMS *Endurance* for their assistance during the 2006-2007 field season, Mark Laidlaw for field
482 assistance and Paul Brickle (Falkland Island Fisheries) for supplying sub-fossil material of *Austrochlamys* from the
483 Falkland Islands. Alistair Crame (BAS) is thanked for permission to analyse the bivalve material geochemically. Colin
484 Cunningham and Rob Wilson (Leicester) made thin sections and helped with SEM photomicrography, respectively. The
485 late Tim Brewer ran analyses of shell geochemistry for us and advised on shell preservation. Cheryl Haidon undertook
486 the XRD analysis of shells. We are especially grateful to Hilary Sloane (NIGL) for assistance with the isotope analysis,
487 to Arne Ghys (Belgium) for supplying comparative modern *Austrochlamys* material from Tierra del Fuego, and to
488 Harry Dowsett (USGS) and Daniel Lunt (Bristol) for their constructive reviews. BRS acknowledges financial support
489 by a DFG (SCHO793/4). This is Geocycles publication number X.

490

491 **References**

- 492 Adam, M.E. 1990. Shell growth in some Nile bivalves. *Journal of Molluscan Studies*, 56, 301-308.
- 493 Berkman, P.A., Cattaneo-Vietti, R., Chiantore, M., Howard-Williams, C. 2004. Polar emergence
494 and the influence of increased sea-ice extent on the Cenozoic biogeography of pectinid molluscs
495 in Antarctic coastal areas. *Deep Sea Research Part 2*, 51, 1839-1855.
- 496 Bigg, G. R., Rohling, E.J. 2000. An oxygen isotope data set for marine waters, *Journal of*
497 *Geophysical Research*, 105, 8527–8535
- 498 Clark II, G.R. 1974. Calcification on an unstable substrate: marginal growth in the mollusk *Pecten*

- 499 diegensis. *Science*, 183, 968-970.
- 500 Clark II, G.R. 2005. Daily growth lines in some living *Pectens* (Mollusca: Bivalvia) and some
501 applications in a fossil relative: Time and tide will tell. *Palaeogeography, Palaeoclimatology,*
502 *Palaeoecology*, 228, 26-42.
- 503 Craig, H. 1965. The measurement of oxygen isotope palaeotemperatures. In: Tongiorgi, E. (Ed.),
504 *Stable Isotopes in Oceanographic Studies and Palaeotemperatures*. Pisa, Consiglio Nazionale
505 delle Ricerche Laboratorio di Geologia Nucleare, pp. 161–182.
- 506 Dame, R.F. 1996. *Ecology of marine bivalves: an ecosystem approach*. CRC Press: Boca Raton,
507 Florida. 254 pp.
- 508 Dijkstra, H.H., Köhler, F. 2008. An annotated catalogue of Recent Pectinoidea (Mollusca,
509 Pectinidae and Propeamussiidae) type material in the Museum of Natural History, Humboldt
510 University, Berlin. *Zoosystematics and Evolution*, 84, 31-44.
- 511 Dijkstra, H.H., Marshall, B.A. 2008. The Recent Pectinoidea of the New Zealand region (Mollusca:
512 Bivalvia: Propeamussiidae, Pectinidae and Spondylidae). *Molluscan Research*, 28, 1-88.
- 513 Dowsett, H.M. 2007. The PRISM palaeoclimate reconstruction and Pliocene sea-surface
514 temperature. In: Williams, M., Haywood, A.M., Gregory, F.J., Schmidt, D.N. (eds.) *Deep-*
515 *Time Perspectives on Climate Change: Marrying the Signal from Computer Models and*
516 *Biological Proxies*. The Micropalaeontological Society, Special Publications, The Geological
517 Society, London, pp. 459-480.
- 518 Epstein, S., Buchsbaum, R., Lowenstam, H.A., Urey, H.C. 1953. Revised carbonate water isotopic
519 temperature scale. *Geological Society of America Bulletin*, 64, 1315–1326.
- 520 Hambrey, M.J., Smellie, J.L., Nelson, A.E., Johnson, J.S. 2008. Late Cenozoic glacier-volcano
521 interaction on James Ross Island and adjacent areas, Antarctic Peninsula region. *Geological*
522 *Society of America Bulletin*, doi: 10.1130/B26242.1.
- 523 Haywood, A.M., Valdes, P.J., Peck, V.L. 2007. A permanent El Niño-like state during the
524 Pliocene? *Paleoceanography*, 22 (1), doi:10.1029/2006PA001323

- 525 Haywood, A.M., Valdes, P.J., Hill, D.J., Williams, M. 2007. The mid-Pliocene warm period: A
526 test-bed for integrating data and models. In: Williams, M., Haywood, A.M., Gregory, F.J.,
527 Schmidt, D.N (eds) Deep time perspectives on climate change: marrying the signal from
528 computer models and biological proxies. The Micropalaeontological Society, Special
529 Publications. The Geological Society, London, 443-457.
- 530 Haywood, A.M., Dowsett, H.J., Valdes, P.J., Lunt, D.J., Francis, J.E., Sellwood, B. 2009. Pliocene
531 climate, processes and problems. *Philosophical Transactions of the Royal Society, Series A*, 367,
532 3-17.
- 533 Hepp, D.A., Mörz, T., Grützner, J. 2006. Pliocene glacial cyclicality in a deep-sea sediment drift
534 (Antarctic Peninsula Pacific Margin). *Palaeogeography, Palaeoclimatology, Palaeoecology*, 231,
535 181-198.
- 536 Hillenbrand, C-D., Fütterer, D.K. 2002. Neogene to Quaternary deposition of opal on the
537 continental rise west of the Antarctic Peninsula, ODP Leg 178, Sites 1095, 1096, and 1101. In:
538 Barker, P.F., Camerlenghi, A., Acton, G.D., Ramsay, A.T.S. (eds) *Proceedings of the Ocean
539 Drilling Programme, Scientific Results*, 178. Texas A and M University, College Station, Texas,
540 1-40 (CD-ROM).
- 541 Jansen, E., Overpeck, J., Briffa, K.R., Duplessy, J.-C., Joos, F., Masson-Delmotte, V., Olago, D.,
542 Otto-Bliesner, B., Peltier, W.R., Rahmstorf, S., Ramesh, R., Raynaud, D., Rind, D., Solomina,
543 O., Villalba, R., Zhang, D. 2007. Palaeoclimate. In: *Climate Change 2007: The Physical
544 Science Basis. Contribution of Working Group I to the Fourth Assessment Report of the
545 Intergovernmental Panel on Climate Change*, Cambridge University Press, Cambridge, United
546 Kingdom and New York, NY, USA.
- 547 Johnson, A.L.A., Hickson, J.A., Swan, J., Brown, M.R., Heaton, T.H.E., Chenery, S., Balson, P.S.
548 2000. The Queen Scallop *Aequipecten opercularis*: a new source of information on late
549 Cenozoic marine environments in Europe. In: Harper, E.M., Taylor, J.D., Crame, J.A. (eds) *The*

- 550 Evolutionary Biology of the Bivalvia. pp. 425-439. Geological Society of London, Special
551 Publications 177.
- 552 Johnson, A.L.A., Hickson, J.A., Bird, A., Schoene, B.R., Balson, P.S., Heaton, T.H.E., Williams,
553 M. 2009. Bivalve sclerochronology and the mid-Pliocene (c. 3.5 Ma) climate of the Southern
554 North Sea Basin. *Palaeogeography, Palaeoclimatology, Palaeoecology*, doi:
555 10.1016/j.palaeo.2009.09.022
- 556 Johnson, J.S., Smellie, J.L., Nelson, A.E., Stuart, F.M. 2009. Did the Antarctic Peninsula Ice Sheet
557 persist during interglacials? – evidence from cosmogenic dating of Pliocene lavas on James
558 Ross Island. *Global and Planetary Change*, doi:10.1016/j.gloplacha.2009.09.001
- 559 Jones, D.S., Allmon, W.D. 1995. Records of upwelling, seasonality and growth in stable-isotope
560 profiles of Pliocene mollusk shells from Florida. *Lethaia*, 28, 61-74.
- 561 Jones, D.S., Quitmyer, I.R. 1996. Marking time with bivalve shells: oxygen isotopes and season of
562 annual increment formation. *Palaios*, 11, 340-346.
- 563 Jonkers, H.A. 1998a. Stratigraphy of Antarctic late Cenozoic pectinid-bearing deposits. *Antarctic
564 Science*, 10, 161-170.
- 565 Jonkers, H.A. 1998b. The Cockburn Island Formation; Late Pliocene interglacial sedimentation in
566 the James Ross Basin, northern Antarctic Peninsula. *Newsletters on Stratigraphy*, 36, 63-76.
- 567 Jonkers, H.A. 2003. Late Cenozoic–Recent Pectinidae (Mollusca: Bivalvia) of the Southern Ocean
568 and neighbouring regions. *Monographs of Marine Mollusca*, 5, 125 pp.
- 569 Jonkers, H.A., Lirio, J.M., Dell Valle, R.A., Kelley, S.P. 2002. Age and environment of Miocene-
570 Pliocene glaciomarine deposits, James Ross Island, Antarctica. *Geological Magazine*, 139, 577-
571 594.
- 572 Knowles, T., Taylor, P.D., Williams, M., Haywood, A.M., Okamura, B. 2009. Pliocene seasonality
573 across the North Atlantic inferred from cheilostome bryozoans. *Palaeogeography,
574 Palaeoclimatology, Palaeoecology*, 277, 226-235

- 575 Krantz, D. E., Williams, D. F., Jones, D. S. 1987. Ecological and paleoenvironmental information
576 using stable isotope profiles from living and fossil molluscs. *Palaeogeography,*
577 *Palaeoclimatology, Palaeoecology*, 58, 249-266.
- 578 Leng, M.J., Marshall, J.D. 2004. Palaeoclimate interpretation of stable isotope data from lake
579 sediment archives. *Quaternary Science Reviews*, 23, 811-831.
- 580 Levitus, S., Boyer, T.P. 1994. *World Ocean Atlas 1994*, vol. 4, Temperature, NOAA Atlas
581 NESDIS, vol. 4, 129 pp., NOAA, Silver Spring, Md.
- 582 Lunt, D.J., Valdes, P.J., Haywood, A.M., Rutt, I. 2008. Closure of the Panama Seaway during the
583 Pliocene – Implications for Climate and Northern Hemisphere Glaciation. *Climate Dynamics*,
584 30, 1-18. (doi:10.1007/s00382-007-0265-6).
- 585 McArthur, J.M., Rio, D., Massari, F., Castradori, D., Bailey, T.R., Thirlwall, M., Houghton, S.
586 2006. A revised Pliocene record for marine- $^{87}\text{Sr}/^{86}\text{Sr}$ used to date an interglacial event recorded
587 in the Cockburn Island Formation, Antarctic Peninsula. *Palaeogeography, Palaeoclimatology,*
588 *Palaeoecology*, 242, 126-136.
- 589 McConnaughey, T.A., Gillikin, D.P. 2008. Carbon isotopes in mollusk shell carbonates. *Geo-*
590 *Marine Letters*, doi:10.1007/s00367-008-0116-4.
- 591 McConnaughey, T.A., Burdett, J., Whelan, J.F., Paull, C.K. 1997. Carbon isotopes in biological
592 carbonates: Respiration and photosynthesis. *Geochimica et Cosmochimica Acta*, 61, 611-622.
- 593 Meredith, M.P., Brandon, M.A., Wallace, M.I., Clarke, A., Leng, M.J., Renfrew, I.A., van Lipzig,
594 N.P.M., King, J.C. 2008. Variability in freshwater balance of northern Marguerite Bay,
595 Antarctic Peninsula: results from $\delta^{18}\text{O}$. *Deep Sea Research Part 2*, 55, 309-322.
- 596 Nelson, A., Smellie, J., Williams, M., Zalasiewicz, J.A. 2008. Late Miocene marine trace fossils
597 from James Ross Island. *Antarctic Science*, 20, 591-592.
- 598 Nelson, A.E., Smellie, J., Hambrey, M., Williams, M., Vautravers, M., McArthur, J., Regelous, M.
599 2009. Neogene glacial debris flows on James Ross Island, northern Antarctic Peninsula, and

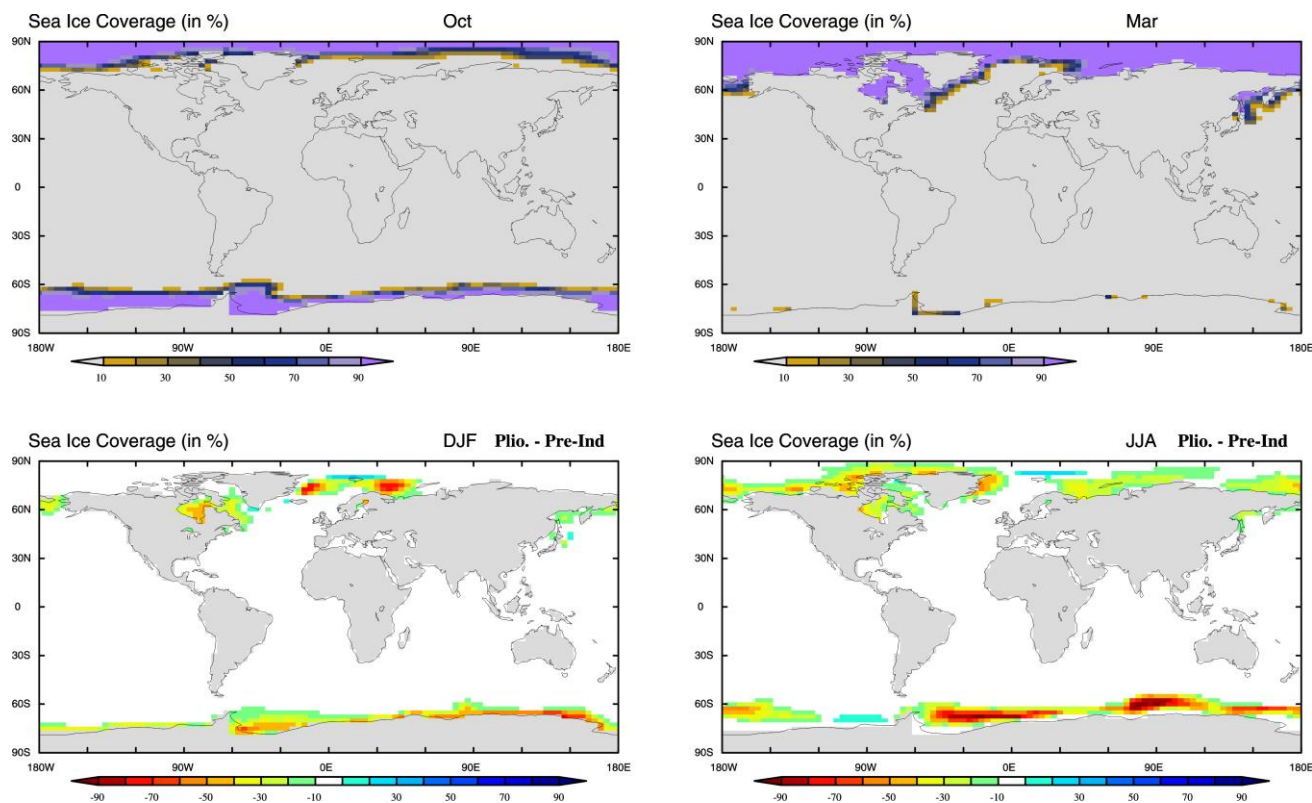
- 600 their implications for regional climate history. *Quaternary Science Reviews*,
601 doi:10.1016/j.quascirev.2009.08.016
- 602 O'Neil, J.R., Clayton, R.N., Mayeda, T.K. 1969. Oxygen isotope fractionation in divalent metal
603 carbonates. *Journal of Chemical Physics*, 51, 5547-58
- 604 Owen, R., Kennedy, H., Richardson, C. 2002a. Experimental investigation into partitioning of
605 stable isotopes between scallop (*Pecten maximus*) shell calcite and sea water. *Palaeogeography*,
606 *Palaeoclimatology, Palaeoecology*, 185, 163-174.
- 607 Owen, R., Richardson, C., Kennedy, H. 2002b. The influence of shell growth rate on striae
608 deposition in the scallop *Pecten maximus*. *Journal of the Marine Biological Association of the*
609 *United Kingdom*, 82, 621-623.
- 610 Pirrie, D., Crame, J.A., Riding, J.B., Butcher, A.R., Taylor, P.D. 1997. Miocene glaciomarine
611 sedimentation in the northern Antarctic Peninsula region: the stratigraphy and sedimentology of
612 the Hobbs Glacier Formation, James Ross Island. *Geological Magazine*, 134, 745-762. doi:
613 10.1017/S0016756897007796.
- 614 Pudsey, C.J. 2002. Neogene record of Antarctic Peninsula glaciation in continental rise sediments:
615 ODP Leg 178, Site 1095. In: Barker, P.F., Camerlenghi, A., Acton, G.D., Ramsay, A.T.S. (eds)
616 *Proceedings of the Ocean Drilling Programme, Scientific Results*, 178. Texas A and M
617 University, College Station, Texas, 1-40 (CD-ROM).
- 618 Quilty, P.G., Murray-Wallace, C.V., Whitehead, J.M. 2004. *Austrochlamys heardensis* (Fleming,
619 1957) (Bivalvia: Pectinidae) from Central Kerguelen Plateau, Indian Ocean: palaeontology and
620 possible tectonic significance. *Antarctic Science*, 16, 329-338.
- 621 Rohling, E. J. 2000. Paleosalinity: Confidence limits and future applications, *Marine Geology*, 163,
622 1–11.
- 623 Rohling, E. J., Bigg, G.R. 1998. Paleo-salinity and $\delta^{18}\text{O}$: a critical assessment, *Journal of*
624 *Geophysical Research*, 103, 1307–1318

- 625 Schöne, B.R., Oschmann, W., Rössler, J., Freyre Castro, A.D., Houk, S.D., Kröncke, I, Dreyer, W.,
626 Janssen, R., Rumohr, H., Dunca, E. 2003. North Atlantic Oscillation dynamics recorded in
627 shells of a long-lived bivalve mollusk. *Geology*, 31, 1037-40.
- 628 Schöne, B.R., Fiebig, J., Pfeiffer, M., Gless, R., Hickson, J., Johnson, A.L.A., Dreyer, W.,
629 Oschmann, W. 2005. Climate records from a bivalved Methuselah (*Arctica islandica*, Mollusca;
630 Iceland). *Palaeogeography, Palaeoclimatology, Palaeoecology*, 228, 130-148.
- 631 Schmidt, G. A. 1998. Oxygen-18 variations in a global ocean model, *Geophysical Research Letters*,
632 25, 1201–1204.
- 633 Schmidt, G.A. 1999. Forward modelling of carbonate proxy data from planktonic foraminifera
634 using oxygen isotope tracers in a global ocean model, *Paleoceanography*, 14, 482–497.
- 635 Schmidt, G.A., Bigg, G.R., Rohling, E.J. 1999. "Global Seawater Oxygen-18 Database".
636 <http://data.giss.nasa.gov/o18data/>
- 637 Smellie, J.L., McArthur, J.M., McIntosh, W.C., Esser, R. 2006a. Late Neogene interglacial events
638 in the James Ross Island region, northern Antarctic Peninsula, dated by Ar/Ar and Sr-isotope
639 stratigraphy. *Palaeogeography, Palaeoclimatology, Palaeoecology*, 242, 169-187.
- 640 Smellie, J.L., Nelson, A.E., Williams, M. 2006b. Fire and ice: unravelling the climatic and volcanic
641 history of James Ross Island, Antarctic Peninsula. *Geology Today*, 22, 220-226.
- 642 Smellie, J.L., Johnson, J.S., McIntosh, W.C., Esser, R., Gudmundsson, M.G., Hambrey, M.J., de
643 Vries, B. Van Wyk. 2008. Six million years of glacial history recorded in the James Ross Island
644 Volcanic Group, Antarctic Peninsula. *Palaeogeography, Palaeoclimatology, Palaeoecology*, 260,
645 122-148.
- 646 Smellie, J.L., Haywood, A.M., Hillenbrand, C-D., Lunt, D.L., Valdes, P.J. 2009. Nature of the
647 Antarctic Peninsula Ice Sheet during the Pliocene: geological evidence and modelling results
648 compared. *Earth-Science Reviews*, 94, 79-94.
- 649 Whitehouse, M.J., Priddle, J., Symon, C. 1996. Seasonal and annual change in seawater temperature,
650 salinity, nutrient and chlorophyll a distributions around South Georgia, South Atlantic. *Deep Sea*

- 651 Research Part 1, 43, 425-443.
- 652 Whitehead, J.M., Bohaty, S.M. 2003. Pliocene summer sea surface temperature reconstruction using
653 silicoflagellates from Southern Ocean ODP Site 1165. *Paleoceanography*, 18, 1075,
654 doi:10.29/2002PA000829.
- 655 Whitehead, J.M., Wotherspoon, S., Bohaty, S.M. 2005. Minimal Antarctic sea ice during the Pliocene.
656 *Geology*, 33, 137-140.
- 657 Witbaard, R. 1996. Growth variations in *Arctica islandica* L. (Mollusca): a reflection of hydrography-
658 related food supply. *ICES Journal of Marine Science*, 53, 981-987
- 659 Williams, M., Smellie, J., Johnson, J., Blake, D. 2006. Late Miocene Asterozoans (Echinodermata)
660 from the James Ross Island Volcanic Group. *Antarctic Science*, 18, 117–122.
- 661 Williams, M., Haywood, A.M., Harper, E.M., Johnson, A., Knowles, T., Leng, M.J., Lunt, D.,
662 Okamura, B., Taylor, P., Zalasiewicz, J.A. 2009a. Pliocene climate and seasonality in North
663 Atlantic shelf seas. *Philosophical Transactions of the Royal Society, London, Series A*, 367, 85-
664 108 (doi:10.1098/rsta.2008.0224)
- 665 Williams, M., Nelson, A.E., Smellie, J.L., Leng, M.J., Jarram, D.R., Johnson, A.L.A., Haywood,
666 A.M., Peck, V.L., Zalasiewicz, J.A., Bennett, C.E., Schöne, B.R. 2009b. A high fidelity
667 molluscan climate record for the Weddell Sea for a warm interval of the Early Pliocene.
668 Workshop on Pliocene climate, Bordeaux, France, October 22nd to 25th 2009. Abstract at:
669 <http://www.plioclimworkshop.com/>

670

671 **Explanation of figures and table**

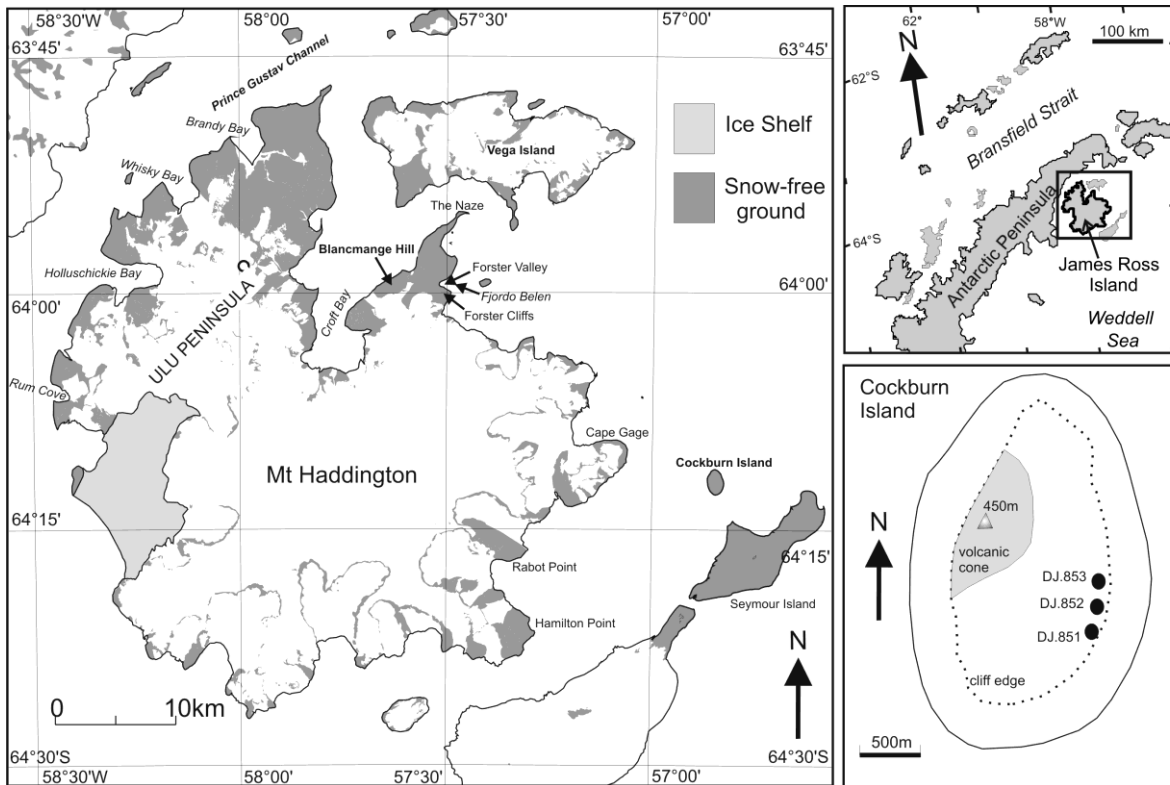


672

673

674 **Fig. 1.** Predictions of absolute sea-ice coverage (%) for maximum (top left) and minimum sea-ice
 675 months (top right) in the Southern Hemisphere for the Early Pliocene (data from Lunt et al.,
 676 2008). The model predicts sea ice coverage in the northern Weddell Sea at 57°W and 64°S as
 677 0.012% cover for late summer rising to 0.908% for late winter. Also shown are the differences
 678 between Early Pliocene and pre-industrial sea-ice cover as an average for the Southern Hemisphere
 679 summer (December, January and February [DJF; bottom left]) and winter seasons (June, July and
 680 August [JJA; bottom right]). Predictions from the Hadley Centre for Climate Research fully
 681 coupled ocean-atmosphere General Circulation Model version 3 (HadCM3).

682

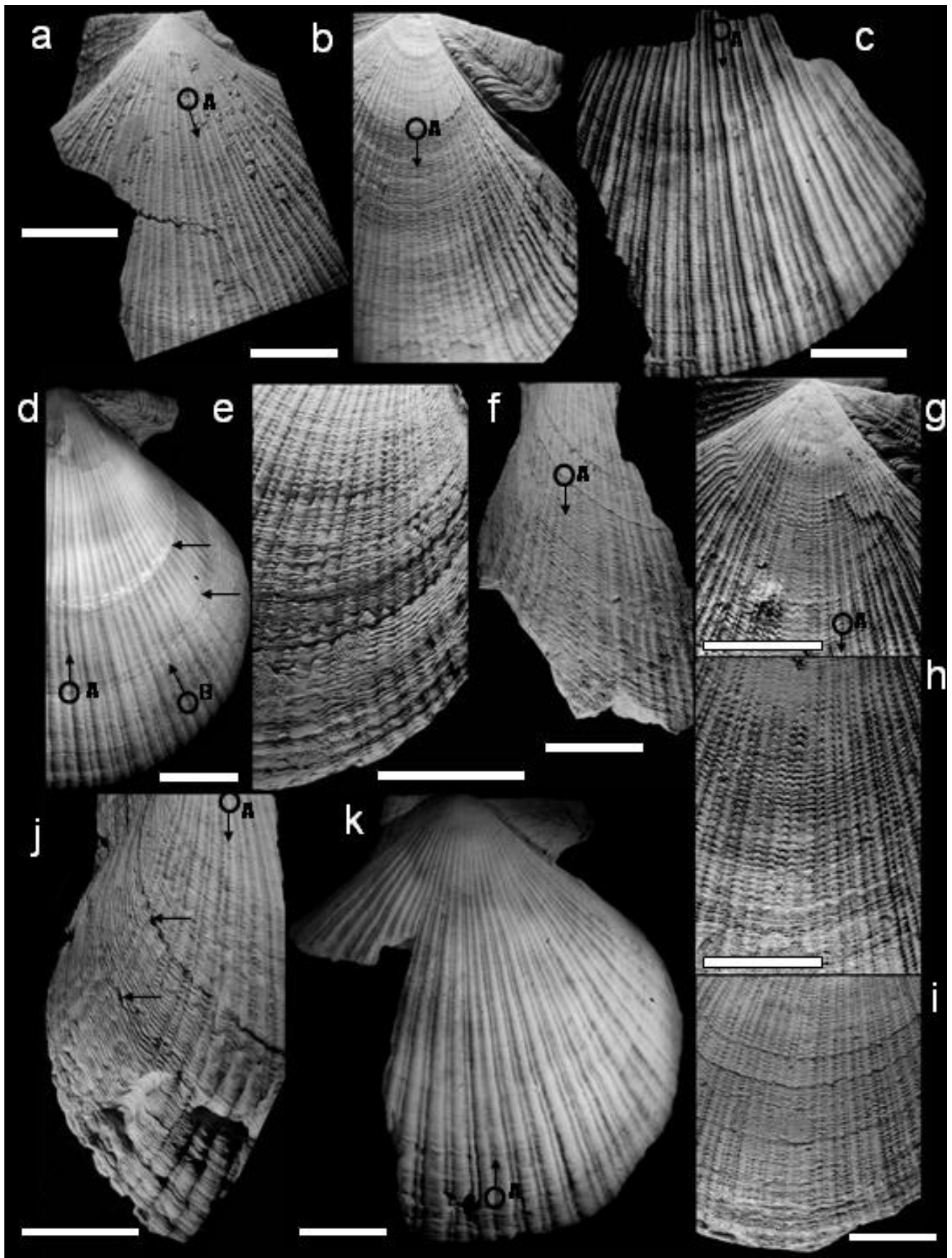


683

684

685 **Fig. 2.** Geographical location of James Ross Island on the northern Antarctic Peninsula (top right)
 686 and Cockburn Island (see main map to the left). Mollusc material for geochemical and
 687 morphological analysis mentioned here is sourced from three localities on the east side of Cockburn
 688 Island (map bottom right, localities DJ.851, DJ.852 and DJ.853 of H.A. Jonkers 1996, for which see
 689 BAS archives). *Austrochlamys* material is also widespread in the glacial sediments of James
 690 Ross Island, for example at northwest Forster cliffs.

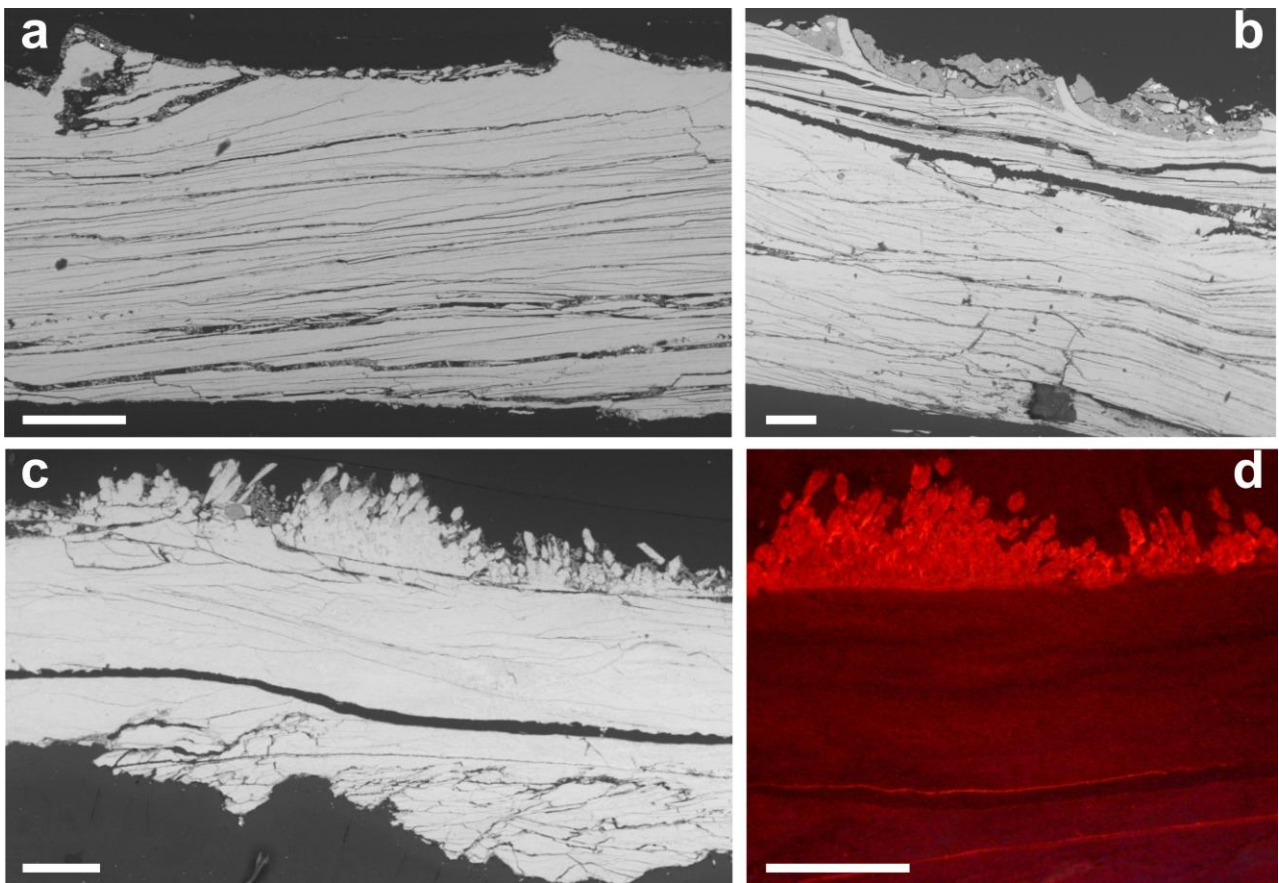
691



692

693 **Fig. 3.** Morphology of the bivalve *Austrochlamys*. The images are annotated with open circles
 694 (labelled 'A' or 'B') to show points on the shell for cross reference with Figures 4 and 6. The arrow

695 points in the direction where increments were measured. Also arrowed are major growth lines on
 696 two of the shells for comparison with the growth/isotope profiles shown in Figure 6. a, right valve,
 697 British Antarctic Survey (BAS) DJ.851.8. b, e, right valve, DJ.851.1. c, unnumbered specimen in
 698 BAS collection. d, right valve, DJ.853.1. f, left valve, DJ.852.22. g-i, right valve, DJ.851.3. j, right
 699 valve, DJ.851.159: bottom right part of image shows damage to the shell possibly as a response to
 700 disturbance by a predator. k, right valve, DJ.852.1. All specimens were collected from Cockburn
 701 Island by H.A. Jonkers and S.L. White in 1996 (see Fig. 2 for localities) except c, which was
 702 collected from surface scree by M. Williams and M. Laidlaw in 2006. Scale bars are 2 cm.
 703



704
 705 **Fig. 4.** SEM images of polished thin sections of two specimens of Pliocene *Austrochlamys* from the
 706 Antarctic Peninsula (a, b). Both images show the well preserved foliated structure of the bivalve
 707 shell, but with a thin layer of sediment adhering to the outer surface that was removed prior to
 708 geochemical analysis. A specimen with an external diagenetic overgrowth cement of calcite
 709 crystals, from the same locality is shown in (c) SEM image, and (d) cathodoluminescence image.

710 The diagenetic cement is brightly luminescent, while the shell foliae are weakly luminescent. Scale
 711 bars are 0.25 mm.
 712

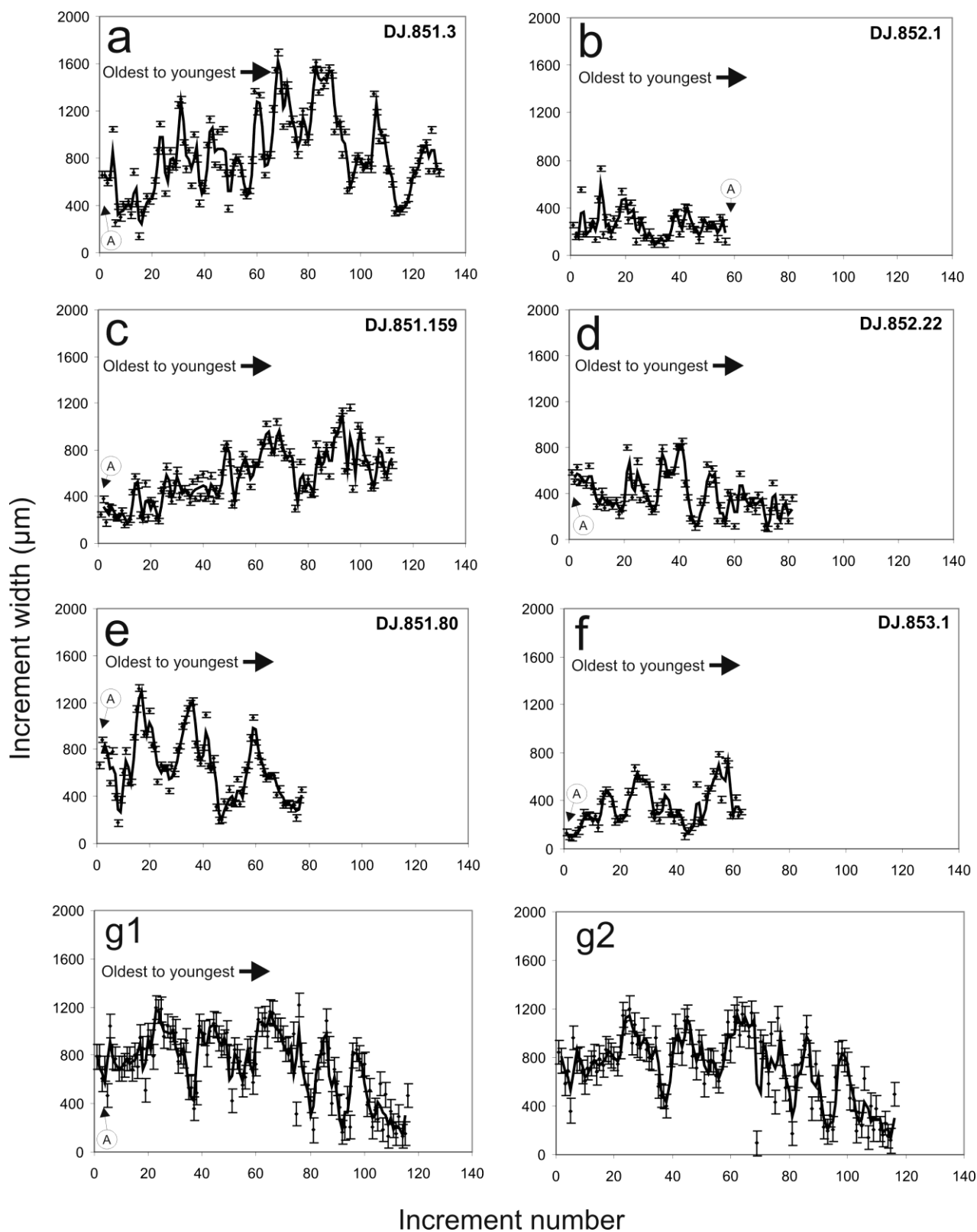
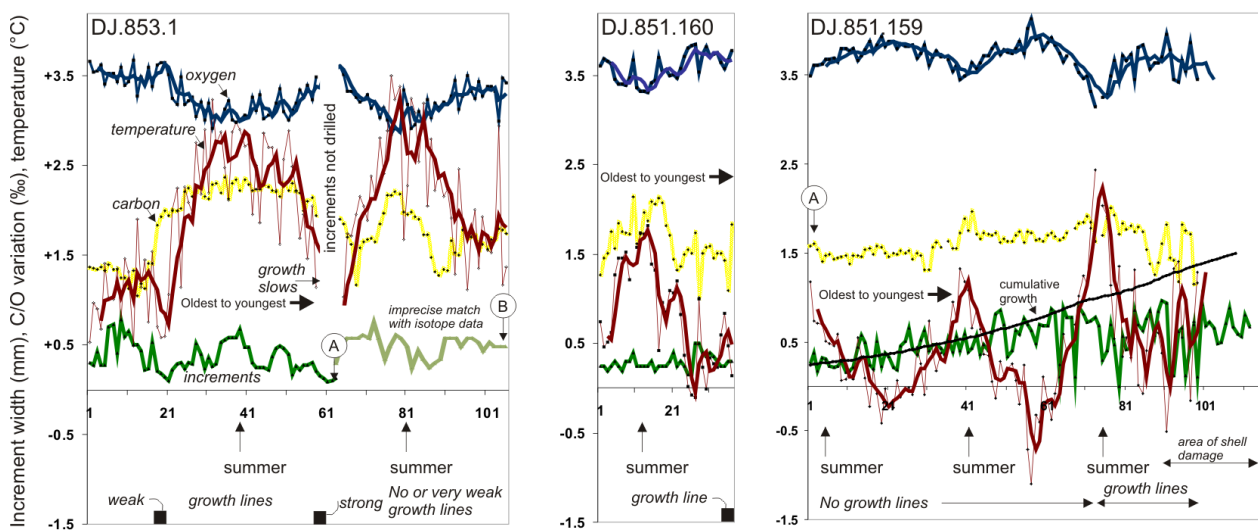


Fig. 5. Growth increment analysis of bivalves from the Cockburn Island Formation. Graphs a-f

715 show growth increments plotted for areas of bivalve shells shown in Figure 3 ('A' denotes points on
 716 the shell for cross-reference). Graphs g1 and g2 show repeat measurements for one shell (Fig. 3c)
 717 demonstrating the accuracy of measurements that can be achieved with Panopea. Vertical scale is
 718 μm , horizontal scale is growth increment measured from oldest (1) to youngest. In addition to the
 719 shells plotted here, over 200 increments measured for shell DJ.851.1 show a similar pattern of high-
 720 frequency growth variation.

721



722

723 **Fig. 6.** Seasonality recorded in the bivalves DJ.851.159, DJ.851.160 and DJ.853.1 from the
 724 Cockburn Island Formation. The figure plots $\delta^{13}\text{C}$ (yellow) and $\delta^{18}\text{O}$ (blue) as per mil variation (left
 725 hand vertical scale). Also shown is temperature (red, left hand scale in $^{\circ}\text{C}$) reconstructed using a
 726 $\delta^{18}\text{O}_{\text{sw}}$ value of -0.2‰ and the O'Neil et al. (1969) equation [$T = 16.9 - 4.38(\delta^{18}\text{O}_{\text{c}} - \delta^{18}\text{O}_{\text{sw}}) +$
 727 $0.10(\delta^{18}\text{O}_{\text{c}} - \delta^{18}\text{O}_{\text{sw}})^2$]; thick red line is the 3-point running average of the temperature
 728 reconstruction. The horizontal scale records growth increment number (oldest to left). For all
 729 bivalves incremental growth (3-point running average, green, see left hand scale mm variation) is
 730 also plotted as is cumulative growth (black line, scale not shown) in bivalve DJ.851.159. 'A' and
 731 'B' denote a point on the shell for cross-reference with Figure 3. Also marked are growth lines, with
 732 annotation where these may relate to damage (disturbance) on shell DJ.851.159. Precise matching
 733 of growth increment measurements with increments drilled for isotopes is not possible, but in most

734 cases we have achieved a match in the data of ± 2 to 3 increments. In shell DJ.853.1 the match
 735 between incremental growth and stable isotope values is less precise beyond increment 62 (as
 736 indicated by the change to light green colour for the increments).

737

Modern northern Weddell Sea seasonality	Pliocene Modelled seasonality (depth 0-5m)	Pliocene Modelled seasonality (depth 95-113m)	Bivalve DJ.851.159 ($\delta^{18}\text{O}_{\text{sw}}$ of -0.2‰)	Bivalve DJ.851.159 ($\delta^{18}\text{O}_{\text{sw}}$ of -0.2‰) Craig equation	Bivalve DJ.851.159 ($\delta^{18}\text{O}_{\text{sw}}$ variable from 0 to -0.4‰)	Bivalve DJ.851.160 ($\delta^{18}\text{O}_{\text{sw}}$ of -0.2‰)	Bivalve DJ.851.160 ($\delta^{18}\text{O}_{\text{sw}}$ of -0.2‰) Craig equation	Bivalve DJ.851.160 ($\delta^{18}\text{O}_{\text{sw}}$ variable from 0 to -0.4‰)	Bivalve DJ.853.1 ($\delta^{18}\text{O}_{\text{sw}}$ of -0.2‰)	Bivalve DJ.853.1 ($\delta^{18}\text{O}_{\text{sw}}$ of -0.2‰) Craig equation	Bivalve DJ.853.1 ($\delta^{18}\text{O}_{\text{sw}}$ variable from 0 to -0.4‰)
-0.1 to 1.99	-1.7 to 3.08	-0.69 to -0.52	-1.1 to 2.5	-0.3 to 2.8	-0.4 to 2	-0.1 to 1.8	0.6 to 2.3	0.6 to 1.1	0.5 to 3.5	1.1 to 3.7	1.2 to 2.8
2.09	4.78	0.17	3.6	3.1	2.4	1.9	1.7	0.5	3	2.6	1.6

738

739 **Table 1.** Reconstructed sea temperatures from the Cockburn Island Formation bivalves compared
 740 with modern and modelled Early Pliocene sea temperature seasonality in the northern Weddell Sea.
 741 Modern temperature variation is from Whitehouse et al. (1996), modelled Early Pliocene data is
 742 from Lunt et al. (2008). Both temperature maxima and minima and total temperature range are
 743 shown. Temperature calculations for ‘Craig (1965)’ use the form of this equation given in Leng and
 744 Marshall (2004) [$T=16-4.14(\delta^{18}\text{O}_{\text{c}} - \delta^{18}\text{O}_{\text{sw}}) + 0.13(\delta^{18}\text{O}_{\text{c}} - \delta^{18}\text{O}_{\text{sw}})^2$] and a $\delta^{18}\text{O}_{\text{sw}}$ value of -0.2‰ .

745

746 **Appendix 1.** Model calculated values for the $\delta^{18}\text{O}$ of seawater are an attempt to capture
 747 longitudinal and latitudinal change as a function of climate, and are based on precipitation minus
 748 evaporation (P – E) estimates derived from the GCM. Present-day observed $\delta^{18}\text{O}_{\text{sw}}$ [Bigg and
 749 Rohling, 2000; Schmidt, 1998, 1999; G. A. Schmidt et al., 1999, Global seawater oxygen-18
 750 database, available at <http://data.giss.nasa.gov/o18data/>] is calibrated against observed P – E
 751 (ECMWF reanalysis data) for the Atlantic Ocean. The resulting formulae (see below) are used to
 752 predict $\delta^{18}\text{O}_{\text{sw}}$.

753

754 Atlantic Calibration:

755

$$756 \delta^{18}\text{O}_{\text{sw}} = 0.24 - 0.008 (P - E) \quad r^2 = 0.7$$

757

758 P - E is given in units of cm yr^{-1} .

759

760 Although this is a useful approach, care must be taken when examining the results since they are
761 based solely on the model's predictions of P - E, where in reality the $\delta^{18}\text{O}_{\text{sw}}$ is also dependent upon
762 mixing because of ocean currents, runoff, etc. The resulting correlation for the Atlantic Ocean
763 $\delta^{18}\text{O}_{\text{sw}}$ to P - E is reasonable. In addition to P - E we calibrated $\delta^{18}\text{O}_{\text{sw}}$ against salinity [Levitus and
764 Boyer, 1994]. This increased the r^2 value to 0.9 for the Atlantic but Haywood et al. (2007)
765 demonstrated that this did not significantly change the diagnostic predictions of $\delta^{18}\text{O}_{\text{sw}}$ generated
766 using P - E for the Pliocene.

767 Nevertheless, it is important to recognise that the use of a salinity: $\delta^{18}\text{O}$ or P - E: $\delta^{18}\text{O}$ co-
768 variation from present-day observations as a diagnostic for the $\delta^{18}\text{O}$ composition of seawater is
769 complicated by the fact that temperature gradients are steeper today than they were during the
770 Miocene and Pliocene (a reflection of cooler temperatures in polar regions today) which will result
771 in different patterns of Rayleigh distillation and hence different $\delta^{18}\text{O}$ values in the hydrological
772 cycle [Rohling and Bigg, 1998; Rohling, 2000].

773

774